

Determination of the Weak Axial Vector Coupling $\lambda = g_A/g_V$ from a Measurement of the β -Asymmetry Parameter A in Neutron Beta Decay

D. Mund,^{*} B. Märkisch,[†] M. Deissenroth, J. Krempel,[‡] M. Schumann,[§] and H. Abele^{||}
Physikalisches Institut, Universität Heidelberg, Philosophenweg 12, 69120 Heidelberg, Germany

A. Petoukhov and T. Soldner[¶]

Institut Laue-Langevin, BP 156, 6, rue Jules Horowitz, 38042 Grenoble Cedex 9, France

(Received 13 April 2012; revised manuscript received 11 January 2013; published 23 April 2013)

We report on a new measurement of the neutron β -asymmetry parameter A with the instrument PERKEO II. The main enhancements are the high neutron polarization of $P = 99.7(1)\%$ from a novel arrangement of supermirror polarizers and reduced background from improvements in beam line and shielding. The leading corrections were thus reduced by a factor of 4, pushing them below the level of statistical error and resulting in a significant reduction of systematic uncertainty compared to our previous experiments. We derive the β -asymmetry parameter $A_0 = -0.11972(45)_{\text{stat}}({}^{+32}_{-44})_{\text{sys}} = -0.11972({}^{+53}_{-65})$ and the ratio of the axial vector to the vector coupling constant $\lambda = g_A/g_V = -1.2761(12)_{\text{stat}}({}^{+9}_{-12})_{\text{sys}} = -1.2761({}^{+14}_{-11})$.

DOI: [10.1103/PhysRevLett.110.172502](https://doi.org/10.1103/PhysRevLett.110.172502)

PACS numbers: 12.15.Ji, 13.30.Ce, 14.20.Dh, 23.40.Bw

The standard model of weak interactions describes the β^- decay of the free neutron $n \rightarrow p + e + \bar{\nu}_e$ as a $V - A$ (vector minus axial vector) interaction. Compared to leptonic decays, it implements two new parameters V_{ud} and λ . The up-down matrix element V_{ud} of the Cabibbo-Kobayashi-Maskawa matrix accounts for quark mixing. It relates the vector coupling constant for quarks to that for leptons $g_V = G_F V_{ud}$, where G_F is the Fermi constant measured in muon decay [1]. The axial current is renormalized by the strong interaction at low energy. This is quantified by the parameter $\lambda = g_A/g_V$, the ratio of the axial vector and vector coupling constants. If the weak interaction is invariant under time reversal, the parameter λ is real. Searches for time reversal violation can be found in Refs. [2,3].

The neutron's lifetime τ is related to the parameters λ and V_{ud} and to the available phase space via

$$\tau^{-1} = C|V_{ud}|^2(1 + 3\lambda^2)f^R(1 + \Delta_R), \quad (1)$$

where $C = G_F^2 m_e^5 / (2\pi^3) = 1.1613 \times 10^{-4} \text{ s}^{-1}$ in $\hbar = c = 1$ units. The phase space factor f^R [4,5] includes the model-independent radiative correction. The model-dependent radiative correction Δ_R is taken from Ref. [6]. Thus, λ can be used to determine either V_{ud} or τ . The standard model requests that the Cabibbo-Kobayashi-Maskawa matrix is unitary, a condition which is experimentally tested at the 10^{-4} level for the first row [7], and unitarity tests are sensitive tools for searches for physics beyond the standard model. Previous determinations of V_{ud} and V_{us} raised questions about the unitarity [8–10]. References [11–13] list further motivations to determine λ and to search for new symmetry concepts in neutron beta decay. In principle, the ratio λ can be determined from QCD lattice gauge theory calculations, but the results vary by up to 30% [11]. The most precise experimental

determination is from the β asymmetry in neutron decay, but previous experimental results are not consistent within their uncertainties [1].

In neutron decay, the probability that an electron is emitted with angle ϑ with respect to the neutron spin polarization vector $\mathbf{P} = \langle \boldsymbol{\sigma} \rangle / \sigma$ is [14]

$$W(\vartheta) = 1 + \frac{v}{c} PA \cos(\vartheta), \quad (2)$$

where v is the electron velocity. A is the parity violating β -asymmetry parameter which depends on λ . Accounting for order 1% corrections for weak magnetism $A_{\mu m}$, $g_V - g_A$ interference, and nucleon recoil, A in Eq. (2) reads [4]

$$A = A_0[1 + A_{\mu m}(A_1 W_0 + A_2 W + A_3/W)], \quad (3)$$

with total electron energy $W = E_e/m_e c^2 + 1$ (end point W_0). The coefficients $A_{\mu m}$, A_1 , A_2 , and A_3 are from Ref. [4], accounting for a different λ convention. For λ real, A_0 is given by

$$A_0 = -2 \frac{\lambda(\lambda + 1)}{1 + 3\lambda^2}. \quad (4)$$

An additional small radiative correction [15] of order 0.1% [16] must be applied.

In this Letter, we present a new value for λ derived from a measurement of the β asymmetry A with the instrument PERKEO II with strongly reduced systematic corrections and uncertainty. It was installed at the PF1B neutron beam position of the Institut Laue-Langevin (ILL) using a highly polarized cold neutron beam. The antineutrino-asymmetry parameter B [17] (see also Ref. [18]) and the proton-asymmetry parameter C [19] have been measured at this beam with the same instrument. Neutrons moderated by a cold source were guided via a neutron guide [20,21] to the experiment and were polarized using two supermirror (SM)

bender polarizers in crossed (X-SM) geometry [22]. An adiabatic fast passage flipper allowed us to invert the neutron spin direction. After a series of baffles for beam shaping, the transversally polarized neutron beam traversed the PERKEO II spectrometer and was absorbed in a beam dump. Two beam line shutters, in front and behind the baffles, served to gain information on background [9,23]. The main component of the PERKEO II spectrometer is a split-pair superconducting 1 T magnet providing $2 \times 2\pi$ electron guidance from the fiducial volume to either one of two plastic scintillators with size $440 \times 160 \text{ mm}^2$ (see Fig. 2 of Ref. [24]). Details on the spectrometer and electron backscatter suppression can be found in Refs. [9,23].

From the measured electron spectra $N_i^\uparrow(E_e)$ and $N_i^\downarrow(E_e)$ in detector $i = 1, 2$ for neutron spin up and down, respectively, we define the experimental asymmetry as a function of electron kinetic energy E_e as

$$A_{\text{exp},i}(E_e) = \frac{N_i^\uparrow(E_e) - N_i^\downarrow(E_e)}{N_i^\uparrow(E_e) + N_i^\downarrow(E_e)}. \quad (5)$$

With Eq. (2) and $\langle \cos(\vartheta) \rangle = 1/2$, A_{exp} is directly related to the asymmetry parameter A :

$$A_{\text{exp}}(E_e) = \frac{1}{2} \frac{v}{c} APf, \quad (6)$$

with neutron polarization P and spin flip efficiency f .

The main experimental errors of this measurement are due to statistics, detector response, neutron spin polarization, and background subtraction; see Table I. The fourfold intensity of the PF1B beam compared to the previous PF1 beam is used to reduce both statistical and systematic uncertainties.

TABLE I. Summary of corrections and uncertainties relative to the beta asymmetry A_0 , $\Delta A_0/A_0$.

Type	Correction (10^{-3})	Uncertainty (10^{-3})
Neutron polarization	3.0	1.0
Spin flip efficiency	0.0	1.0
Background	1.0	1.0
Detector response	0.0	2.5
Edge effect ^a	(-1.6)	0.5
Electron backscattering (detectors)	0.25	0.04
Electron backscattering (baffles)	0.0	+0.6, -0.0
Magnetic mirror effect	0.6	0.2
Dead time ^b	(-1.2)	0.1
Radiative correction	-1.1	0.5
Systematics (total)	0.95	+3.6, -2.7
Statistics		3.8

^aIncluded in the fit function.

^bMeasured by the data acquisition system and accounted for in the data set.

Polarization.—The X-SM geometry [22] efficiently suppresses garland reflections, resulting in a nearly wavelength- and angle-independent beam polarization. This dramatically reduces systematic uncertainties for determining the average beam polarization. Polarization measurements were performed employing time of flight behind a chopper to gain wavelength resolution. A second adiabatic fast passage flipper and two Schärpf polarizers [25,26] in X-SM geometry as analyzers were used to measure the spin flip efficiency and for a rough determination of the beam polarization. Measurements in front of and behind the PERKEO II spectrometer yielded consistent results. The absolute polarization was determined using a series of opaque ^3He spin filter cells of different pressures and lengths, covering the wavelength range from 2 to 20 Å; see Fig. 1. Cells with both orientations of the ^3He spin were used to increase sensitivity [27]. The wavelength averages were calculated taking into account the decay probability which is proportional to the capture spectrum. The spatial dependence was found to be negligible by measurements at five different positions across the neutron beam. The resulting averages were $P = 99.7(1)\%$ and $f = 100.0(1)\%$ (compared to $P = 98.9(3)\%$ and $f = 99.7(1)\%$ in the previous measurement [9]). The stated errors stem from the conservatively rounded up uncertainties due to statistics, wavelength, and spatial averaging. Note that opaque ^3He spin filters have an intrinsic accuracy of better than 10^{-4} for polarization analysis [28]. We do not use the additional information from the physical boundary $f \leq 1$ to reduce the uncertainty of the spin flip efficiency. This would introduce a bias of the order of the uncertainty, but our uncertainty is conservative, and independent measurements [28] with identical flippers indicate that $|1 - f| < 10^{-4}$.

Background.—The magnetic field of PERKEO II collects all electrons from the decay volume ($100 \times 80 \times 270 \text{ mm}^3$) and thus assures a high signal-to-background ratio,

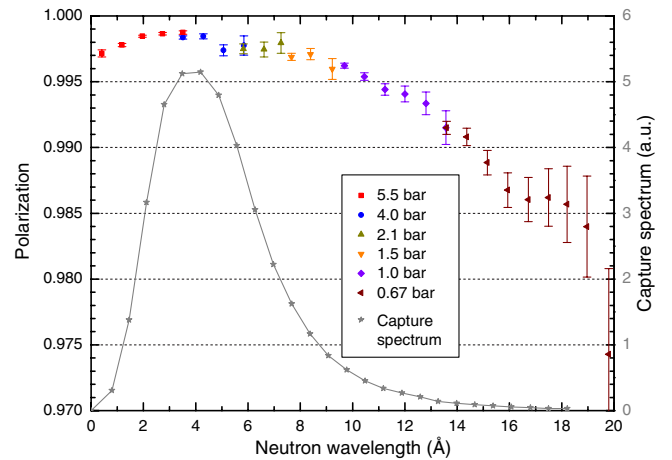


FIG. 1 (color online). Neutron polarization in the center of the PERKEO II beam. The ^3He cells had lengths of 25 or 10 cm. In the legend, the effective pressures for a 10 cm cell are given.

together with thin plastic scintillators (5 mm thickness). Environmental background was reduced by lead and iron shielding and measured with the first beam line shutter closed. It was not constant in time due to shutter operations of neighboring instruments. Changes were monitored by NaI scintillators placed outside the PERKEO II shielding, and shutter operations were registered. For the analysis, only data sets with constant environmental background were used. This reduces the data set to 5.9×10^7 neutron decay events and increases the statistical error to 3.8×10^{-3} (compared to 2.6×10^{-3} in the preliminary analysis of Refs. [11,29]; all errors and corrections quoted in units of 10^{-3} are relative to A_0). The trigger rate of 500 s^{-1} comprises about 120 s^{-1} from environmental background, compared to 375 s^{-1} electrons from neutron decay. The signal-to-background ratio in the fit region was better than 8:1.

Beam-related background is more difficult to address. In the PERKEO II spectrometer, the β detectors are far off the beam at a transverse distance of 960 mm. The beam line was optimized to place the last beam-defining baffle further away from the spectrometer than in our previous measurement [9]. The beam stop was positioned 4 m downstream of the decay volume. The baffles and beam stop were made from enriched ^6LiF ceramics with lead backings. The supports and beam line were protected against scattered neutrons by ^6LiF rubber or boron glass. Halo baffles (not touching the beam) absorbed scattered neutrons close to the beam. Lead shielding was placed around the spectrometer to assure that gamma rays are scattered at least twice before they can reach a detector. Fast neutrons produced by (t, n) reactions in ^6LiF (about 10^{-4} per capture [30]) were shielded by borated polyethylene (or, inside the beam stop vacuum, Plexiglas surrounded by borated glass) and secondary gammas by lead. The beam-related background was estimated from measurements with the two shutters using an extrapolation procedure described in Ref. [24] and confirmed by additional tests with external background sources and a modified beam stop. Compared to the previous measurement [9] of $1/200$, it was reduced to $1/1700$ of the electron rate in the fit region, which corresponds to $0.11(2) \text{ s}^{-1}$ (see Fig. 2), resulting in a correction of $1(1) \times 10^{-3}$. We consider the uncertainty of 100% of this correction as a conservative estimate for the extrapolation method.

Detector response.—The plastic scintillators were read out by four photomultipliers per detector. Signals were integrated by charge-to-digital converters over a time interval that includes signals from backscattering. Trigger time differences between the detectors were registered to identify the detector that triggered first in the case of backscattering. The detector response function was determined and the detector stability checked regularly using four monoenergetic conversion electron sources (^{109}Cd , ^{113}Sn , ^{207}Bi , and ^{137}Cs) on $10 \mu\text{g}/\text{cm}^2$ carbon backings.

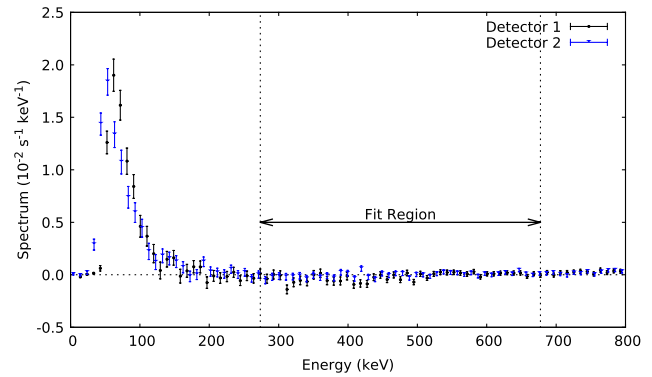


FIG. 2 (color online). Difference of the spectra with the second beam line shutter closed and with the first beam line shutter closed, a measure for the background produced by the collimation system. The main part of the background is low energetic.

The branching ratios of the conversion and Auger electrons, measured using the method described in Ref. [31], were accounted for in the fit functions. Drift in the detector gain was smaller than 1% and corrected for. The detectors showed a small nonlinearity at low energy. In the fit region for the asymmetry parameter A , the effects of the nonlinearity were negligible. The largest systematic uncertainty is caused by the spatial nonuniformity of the detector response. The light collection efficiency from the center of the scintillator was about 5% lower than from the ends. This spatial dependence was mapped using a ^{207}Bi calibration source and was found to follow the expected cosh dependence. The detector calibration, needed for the fit to the asymmetry parameter A of Eq. (6) and Fig. 4, was obtained by a fit to the spectrum $(N^1 - N^4)$ (see Fig. 3),

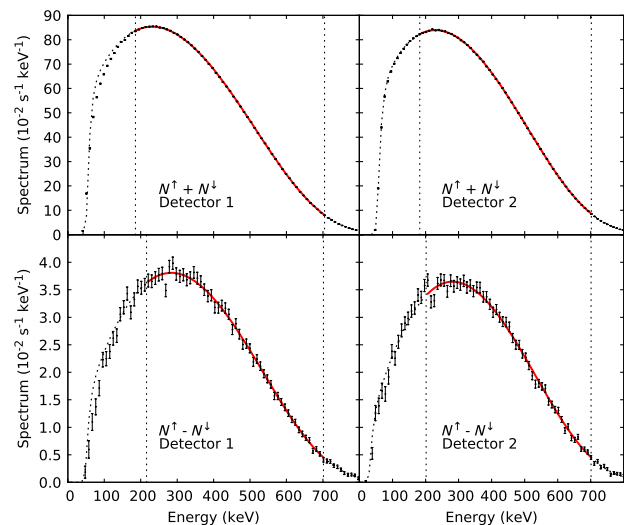


FIG. 3 (color online). Neutron β^- spectra after adding or subtracting opposite neutron spin orientations N^1 and N^4 for detector 1 and detector 2, respectively. The solid curves show fits in the indicated ranges, and the dotted curves show their extrapolations. The spectra $(N^1 - N^4)$ are intrinsically free of (spin-independent) background.

which is background free. A fit to $(N^\uparrow + N^\downarrow)$ would yield a different calibration, resulting in a significant dependence of the asymmetry A on the lower limit of the fit region for detector 2. This might be caused by limited knowledge of low-energy background in the fit region to $(N^\uparrow + N^\downarrow)$; see also Fig. 2. The uncertainty due to the detector response given in Table I accounts for spatial dependence, nonlinearity, and uncertainty of calibration with the spectrum $(N^\uparrow - N^\downarrow)$.

Edge effect.—The length of the decay volume is defined by electron absorbing aluminum baffles. The effective length depends on the radius of gyration. The resulting correction can be calculated from the energy and angular distribution of the electrons and is included in the fit function. The uncertainty accounts for imperfect absorption and uncertainties in the geometry.

Backscattering from detectors and baffles.—By using the second detector as a veto detector and analyzing events with energies below the trigger threshold on one detector [32], the fraction of wrongly attributed electrons in the fit region was deduced to be $1.3(3) \times 10^{-4}$ per detector, corresponding to a correction of $0.25(4) \times 10^{-3}$ compared to $2.0(1.7) \times 10^{-3}$ in the previous experiment [9]. If the electron absorbing aluminum baffles for the two detectors are not well aligned, backscattered electrons can reach the wrong detector. Monte Carlo simulations using GEANT4 [33] show that this effect is smaller than 0.6×10^{-3} (68% C.L.) and would only decrease the absolute value of the measured asymmetry.

Mirror effect.—Electrons can be reflected on an increasing magnetic field, leading to detection in the wrong detector. This magnetic mirror effect, due to a small displacement between the neutron beam and the maximum of the magnetic field, caused a difference of 1.4% between the asymmetries measured in the two detectors. Most of this effect cancels by averaging the two detectors. The remaining correction due to the spatial extension of the neutron beam was calculated from the measured magnetic field geometry and neutron beam profile.

The experimental function $A_{\text{exp},i}(E_e)$ and a fit with a single free parameter λ are shown in Fig. 4 for both detectors. The fit interval was chosen such as to minimize effects due to the nonlinearity of the detector and unrecognized background. The results were independent of the particular choice of the fit interval and stable over time. From the experimental asymmetries, we get $|A_0| = 0.11846(64)_{\text{stat}}$ for detector 1 and $|A_0| = 0.12008(64)_{\text{stat}}$ for detector 2. All subsequent corrections and uncertainties entering the determination of A_0 are listed in Table I. After averaging and correcting for those small and mostly experimental systematic effects, we obtain

$$A_0 = -0.11972(45)_{\text{stat}} \left(\begin{smallmatrix} +32 \\ -44 \end{smallmatrix} \right)_{\text{sys}} = -0.11972 \left(\begin{smallmatrix} +53 \\ -65 \end{smallmatrix} \right) \quad \text{and} \\ \lambda = -1.2761(12)_{\text{stat}} \left(\begin{smallmatrix} +9 \\ -12 \end{smallmatrix} \right)_{\text{sys}} = -1.2761 \left(\begin{smallmatrix} +14 \\ -17 \end{smallmatrix} \right). \quad (7)$$

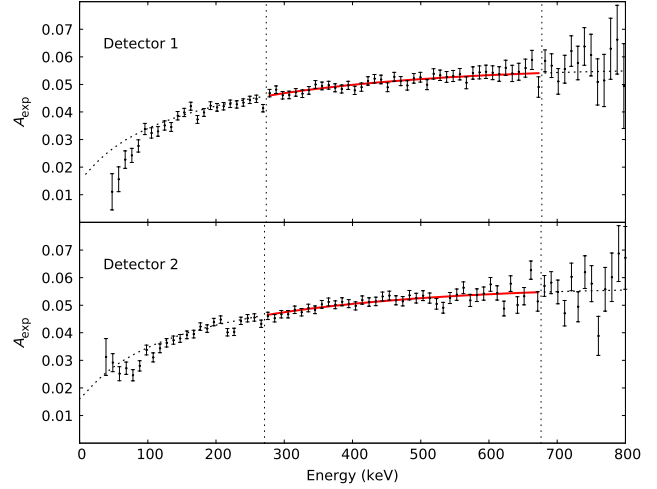


FIG. 4 (color online). Fit to the experimental asymmetry A_{exp} for detector 1 ($\chi^2/\text{dof} = 64/83$) and detector 2 ($\chi^2/\text{dof} = 82/81$), with solid and dotted curves as in Fig. 3.

This value is consistent with our earlier result $A_0 = -0.1187(7)$ [9,23], where we now correct a sign error in the application of radiative corrections to the beta asymmetry. The combined results of all PERKEO II measurements of the beta asymmetry are

$$A_0 = -0.11926(31)_{\text{stat}} \left(\begin{smallmatrix} +36 \\ -42 \end{smallmatrix} \right)_{\text{sys}} = -0.11926 \left(\begin{smallmatrix} +47 \\ -53 \end{smallmatrix} \right) \quad \text{and} \\ \lambda = -1.2748(8)_{\text{stat}} \left(\begin{smallmatrix} +10 \\ -11 \end{smallmatrix} \right)_{\text{sys}} = -1.2748 \left(\begin{smallmatrix} +13 \\ -14 \end{smallmatrix} \right). \quad (8)$$

The average Eq. (8) accounts for correlations of systematic errors in the experiments. Conservatively, errors concerning detector calibration and uniformity, background determination, edge effect, and the radiative correction were considered correlated on the level of the smallest error of all three experiments.

Other experiments [34–36] gave significantly lower values for $|\lambda|$. However, in these experiments, large corrections of 15% to 30% had to be applied for neutron polarization, magnetic mirror effects, solid angle, or background. In our present experiment, all individual corrections are below 3×10^{-3} , and the sum of their absolute values is below 1%. We therefore use only the value given in Eq. (8) for further discussion. The determination of $\lambda = -1.2756(30)$ by the UCNA Collaboration [37] is in agreement with this result.

Assuming the $V - A$ structure of the standard model, the neutron lifetime τ_n can be determined using the $\overline{\mathcal{F}t}$ value from nuclear beta decay

$$\tau_n = \frac{2}{\ln 2} \frac{\overline{\mathcal{F}t}}{f^R(1 + 3\lambda^2)}. \quad (9)$$

Using $f^R = 1.71385(34)$ [5], $\overline{\mathcal{F}t} = 3071.81(83)$ [7], and our result [Eq. (8)], we obtain

$$\tau_n = 880.2 \left(\begin{smallmatrix} +1.5 \\ -1.6 \end{smallmatrix} \right) \text{ s}. \quad (10)$$

This result is in agreement with and nearly as precise as the current world average $\tau_n = 880.1(1.1)$ s [1] that includes a scale factor of 1.8.

The authors thank Dirk Dubbers for his constant support and advice, Andrei Ivanov, Mario Pitschmann [38] and Heiko Saul for compiling the radiative corrections, Markus Brehm for his contribution during the preparation of the measurement, Anthony Hillaret for his contribution during the beam time, Christoph Roick for his backscattering simulations, and several services of the Physikalisches Institut, University of Heidelberg, and of the ILL, in particular, the Neutron Optics Group. This work was supported by the Priority Programme SPP 1491 of the Austrian FWF and the German DFG, Contracts No. FWF I529-N20, No. MA 4944/1-1, and No. SO 1058/1-1, and the German BMBF, Contract No. 06HD187.

*New family name: Schirra.

†maerkisch@physi.uni-heidelberg.de

‡Present address: ETH Zürich, Institut für Teilchenphysik, Schafmattstrasse 20, 8093 Zürich, Switzerland.

§Present address: AEC, Universität Bern, Sidlerstrasse 5, 3012 Bern, Switzerland.

||Present address: Atominstytut, Technische Universität Wien, Stadionallee 2, 1020 Wien, Austria.

abele@ati.ac.at

¶soldner@ill.fr

- [1] J. Beringer *et al.* (Particle Data Group), *Phys. Rev. D* **86**, 010001 (2012).
- [2] T. Soldner, L. Beck, C. Plonka, K. Schreckenbach, and O. Zimmer, *Phys. Lett. B* **581**, 49 (2004).
- [3] H. P. Mumm *et al.*, *Phys. Rev. Lett.* **107**, 102301 (2011).
- [4] D. H. Wilkinson, *Nucl. Phys.* **A377**, 474 (1982).
- [5] G. Konrad, W. Heil, S. Baeßler, D. Pocanic, and F. Glück, in *Proceedings of the 5th International Beyond 2010 Conference, Cape Town, South Africa, 2010* (World Scientific, Singapore, 2011), pp. 660–672.
- [6] W. J. Marciano and A. Sirlin, *Phys. Rev. Lett.* **96**, 032002 (2006).
- [7] J. C. Hardy and I. S. Towner, *Phys. Rev. C* **79**, 055502 (2009).
- [8] I. S. Towner, E. Hagberg, J. C. Hardy, V. Koslowsky, and G. Savard, [arXiv:nucl-th/9507005](https://arxiv.org/abs/nucl-th/9507005).
- [9] H. Abele, M. Astruc Hoffmann, S. Baeßler, D. Dubbers, F. Glück, U. Müller, V. Nesvizhevsky, J. Reich, and O. Zimmer, *Phys. Rev. Lett.* **88**, 211801 (2002).
- [10] *Proceedings of the Two-Day-Workshop “Quark-Mixing, CKM-Unitarity,” Heidelberg, Germany, 2002*, edited by H. Abele and D. Mund (Mattes-Verlag, Heidelberg, 2003).
- [11] H. Abele, *Prog. Part. Nucl. Phys.* **60**, 1 (2008).
- [12] N. Severijns and O. Naviliat-Cuncic, *Annu. Rev. Nucl. Part. Sci.* **61**, 23 (2011).
- [13] D. Dubbers and M. G. Schmidt, *Rev. Mod. Phys.* **83**, 1111 (2011).
- [14] J. D. Jackson, S. B. Treiman, and H. W. Wyld, *Phys. Rev.* **106**, 517 (1957).
- [15] R. T. Shann, *Nuovo Cimento Soc. Ital. Fis.* **5A**, 591 (1971).
- [16] F. Glück and K. Toth, *Phys. Rev. D* **46**, 2090 (1992).
- [17] M. Schumann, T. Soldner, M. Deissenroth, F. Glück, J. Krempel, M. Kreuz, B. Märkisch, D. Mund, A. Petoukhov, and H. Abele, *Phys. Rev. Lett.* **99**, 191803 (2007).
- [18] M. Kreuz *et al.*, *Phys. Lett. B* **619**, 263 (2005).
- [19] M. Schumann, M. Kreuz, M. Deissenroth, F. Glück, J. Krempel, B. Märkisch, D. Mund, A. Petoukhov, T. Soldner, and H. Abele, *Phys. Rev. Lett.* **100**, 151801 (2008).
- [20] H. Häse, A. Knöpfler, K. Fiederer, U. Schmidt, D. Dubbers, and W. Kaiser, *Nucl. Instrum. Methods Phys. Res., Sect. A* **485**, 453 (2002).
- [21] H. Abele *et al.*, *Nucl. Instrum. Methods Phys. Res., Sect. A* **562**, 407 (2006).
- [22] M. Kreuz, V. Nesvizhevsky, A. Petoukhov, and T. Soldner, *Nucl. Instrum. Methods Phys. Res., Sect. A* **547**, 583 (2005).
- [23] H. Abele *et al.*, *Phys. Lett. B* **407**, 212 (1997).
- [24] J. Reich, H. Abele, M. Astruc, Hoffmann, S. Baeßler, P.v. Bülow, D. Dubbers, V. Nesvizhevsky, U. Peschke, and O. Zimmer, *Nucl. Instrum. Methods Phys. Res., Sect. A* **440**, 535 (2000).
- [25] O. Schaerpf, *Physica (Amsterdam)* **156B–157B**, 639 (1989).
- [26] O. Schärpf and N. Stüsser, *Nucl. Instrum. Methods Phys. Res., Sect. A* **284**, 208 (1989).
- [27] O. Zimmer, *Phys. Lett. B* **461**, 307 (1999).
- [28] T. Soldner *et al.*, Institut Laue-Langevin Report No. 3-07-235, 2011.
- [29] D. Mund, Dr. rer. nat. dissertation, Universität Heidelberg, 2006.
- [30] M. Lone, D. Santry, and W. Inglis, *Nucl. Instrum. Methods Phys. Res.* **174**, 521 (1980).
- [31] H. Abele, G. Helm, U. Kania, C. Schmidt, J. Last, and D. Dubbers, *Phys. Lett. B* **316**, 26 (1993).
- [32] M. Schumann and H. Abele, *Nucl. Instrum. Methods Phys. Res., Sect. A* **585**, 88 (2008).
- [33] V. Ivanchenko *et al.*, *Prog. Nucl. Sci. Tech.* **2**, 898 (2011).
- [34] B. Yerozolimsky, I. Kuznetsov, Y. Mostovoy, and I. Stepanenko, *Phys. Lett. B* **412**, 240 (1997).
- [35] P. Liaud, K. Schreckenbach, R. Kossakowski, H. Nastoll, A. Bussière, J. P. Guillaud, and L. Beck, *Nucl. Phys.* **A612**, 53 (1997).
- [36] P. Bopp, D. Dubbers, L. Hornig, E. Klemt, J. Last, H. Schütze, S. Freedman, and O. Schärpf, *Phys. Rev. Lett.* **56**, 919 (1986).
- [37] M. P. Mendenhall *et al.* (UCNA Collaboration), [arXiv:1210.7048](https://arxiv.org/abs/1210.7048).
- [38] A. N. Ivanov, M. Pitschmann, and N. I. Troitskaya, [arXiv:1212.0332](https://arxiv.org/abs/1212.0332).